SEMARAK ILMU PUBLISHING

Journal of Advanced Research in Applied Sciences and Engineering Technology

Journal homepage: https://semarakilmu.com.my/journals/index.php/applied_sciences_eng_tech/index

ISSN: 2462-1943

Element Free Galerkin (EFG) Formulation in Solving Kinematic Wave Equation for Hydrological Modelling

Amrit Singh[1], Halinawati Hirol[1,*], Ahmad Razin Zainal Abidin[2], Mohd Akbar Mohd Noor[3], Mokhtazul Haizad Mokhtaram[3], Airil Yasreen Mohd Yassin[4]

[1] Malaysia-Japan International Institute of Technology (MJIIT), Universiti Teknologi Malaysia, Jalan Sultan Yahya Petra, 54100 Kuala Lumpur, Malaysia
[2] School of Civil Engineering, Faculty of Engineering, Universiti Teknologi Malaysia, 81310 Skudai, Johor, Malaysia
[3] Department of Engineering, Faculty of Engineering and Life Sciences, Universiti Selangor, 45600 Bestari Jaya, Selangor, Malaysia
[4] School of Energy, Geoscience, Infrastructure and Society, Heriot-Watt University Malaysia, 62200, Putrajaya, Malaysia

ARTICLE INFO

Article history:
Received 24 June 2023
Received in revised form 10 October 2023
Accepted 2 November 2023
Available online 16 January 2024

Keywords:
MeshFree method; kinematic wave model; flood routing; hydrological modelling; element free galerkin; saint venant; meshless method

ABSTRACT

Meshfree methods such as Element Free Galerkin Method (EFG) are the cutting edge of numerical methods as it does not require user to perform meshing which often is time consuming and tedious. The method being "meshfree" for the user can theoretically generate more accurate models which follow more complex boundary conditions such as natural rivers etc. The time saving and potential of higher accuracy in modelling makes EFG formulation an interesting research topic. EFG formulation is used to solve kinematic wave equations which is detailed in this paper. Galerkin weighted residual method using EFG's shape function parameters is used to discretize the partial differential equation (PDE) of kinematic wave equations. To discretize the equations, a forward difference scheme is used for temporal discretization and Picard direct substitution method is employed to solve the nonlinear system at each time step. The formulations are validated by making a comparison between well-established numerical techniques against actual recorded datasets. After which it is found that EFG method agrees with conventional established techniques, thus validating the formulations as useful. To further investigate the usefulness of this formulation, an optimal performance study was also conducted to determine the most optimal shape function parameters. The optimal shape function values improved the performance to where it was found that established methods such as FDM were surpassed and on par with FEM. This shows that EFG is a good alternative for hydrological modelling.

1. Introduction

In the 19th century a French monk named Saint-Venant discovered that hydrological phenomenon of channel flow and surface runoff can be measured and predicted. The preceding discovery led to St. Venant equations which essentially are a set of one-dimensional continuity and momentum equations which in its full form are nonlinear and unsteady. Full St. Venant equations can also be

* *Corresponding author.*
E-mail address: halinawati@utm.my

https://doi.org/10.37934/araset.37.2.113

called dynamic wave equations can describe flow fully inclusive of backwater flow when its diffused version equation is used. However, backwater is not always needed hence, the equation can be simplified for easier calculations. If the frictional bed and slope is assumed similar this allows the momentum equation to be simplified and the new equation (simplified version) is known as the Manning equation. The combination of simplified momentum equations (Manning equation) and continuity equation's resultant is known as the kinematic wave equation.

Full St. Venant equation (aka dynamic wave equations) does describe flow more completely. However, its complexity and difficulty in solving it is unnecessary for most cases. Therefore, in order to simplify and reduce the computational costs, the kinematic wave equation is used which is also more stable. This makes the kinematic wave equation more favourable to solve hydrological problems according to Singh [1]. At present, kinematic wave equation has a diverse ability to solve problems ranging from watershed runoff, flood routing, channel flow, erosion to sediment transport. Similar to the full form of St. Venant equation, kinematic wave equations are still unsteady and nonlinear but at a lower magnitude. This nonlinearity still makes obtaining a closed form solution with exact solutions a difficult task. Only in cases where simplified assumptions can be made, can exact solutions be found such as by Parlange *et. al.,* [2], Hjelmfelt [3] and Govindaraju *et. al.,* [4,5]. As kinematic wave is nonlinear, it must be solved by techniques such as finite difference method (FDM) Chow *et. al.,* [6] or finite element method as by Vieux *et. al.,* [7] and Litrico *et. al.,* [8].

2. Element Free Galerkin (EFG): A Meshfree Method

FDM and FEM are numerical methods which are well established methods to solve for kinematic wave equations. However, these techniques require the construction of a mesh or grid to model the physical domain of the intended stimulated problem. Mesh construction is a tedious and difficult process translating into higher costs and time to solve an engineering problem. Innovations to develop meshfree methods are made to help overcome these challenges. Meshfree methods do not require the user to generate a mesh which could seems promising for cheaper and faster problem-solving process by Liu [9], Liu *et al.,* [10].

Meshfree methods refer to a large family of methods which can be used to solve kinematic wave equations. For this paper only Element Free Galerkin (EFG) is considered. EFG is a meshfree method which uses moving least squares (MLS) shape functions to interpolate functions. Belytschko *et. al.,* [11] was the first to propose EFG and showed that EFG is not affected by irregularities during node distribution. EFG now is used for solving multiple problems in linear to nonlinear solvers from 2 to 3 dimensional problems Belytschko *et. al.,* [12], Krsyl and Belytschko [13], Chen *et. al.,* [14]. This study finds that EFG method has relatively good performance on par with FEM with higher convergence rate and higher accuracy.

The application of EFG method in hydrological modelling of flood routing has been detailed in Hirol [15] and Hirol *et. al.,* [16]. However, the challenge of using EFG formulation is the lack of Kronecker delta property, this leads to weak satisfaction of boundary conditions. To overcome this, Langrange multiplier method is hence used to partially satisfy the imposition of the boundary conditions. However, in recent developments it is found that replacing the Dirichlet boundary condition with Robin boundary condition leads to similar efficiency and accuracy with error estimate easily obtainable which cannot be obtained using Dirichlet boundary condition by Dehghan and Abbaszadeh [17]. In other study by Dehghan and Abbaszadeh [17] it is also found that to improve EFG a variational multiscale EGF (VMEFG) can be used which uses moving Kringing interpolation instead of moving least squares thus mitigating many of the problems related to MLS in EFG method. Chowdhury *et. al.,* [18] also introduced modified moving least squares approximation (MMLS) which provide the consistency and invariance properties which are important for accurate computation of shape functions using translation and scaling to a canonical domain. Compared to classical EFG using linear base function, MMLS EFG using quadratic base function provides simulation results which are superior while using the same nodal distribution and support domain size. Zeifang and Schütz [19] found that by combining spatial discretization of discontinuous Galerkin method with implicit two-derivative deferred correction time discretization, nonlinear PDEs can be solved with higher accuracy and convergence rate. Otherwise, attempts have also been made to solve nonlinear Schrödinger equation with EFG using explicit schemes to linearize time convergence by Li and Li [20]. This shows the potential of EFG in handling nonlinear schemes.

In more recent years, more research is concentrated for using meshfree methods such as EFG for real world applications. For example, Smith *et. al.,* [21] used EFG meshfree formulation for plastic stretch blow moulding which was validated against experimental values from manufacturing process of plastic polymer bottles. It was found that the formulation handles can handle rapidly fluctuating values well such as plastic deformation. Which is especially useful for kinematic modelling for river flow upstream to downstream.

3. Methodology

3.1 Governing Equations of Kinematic Wave Equation

St. Venant equations by Saint-Venant [22] depend on time partial differential equations to describe the distribution of flow rate, Q and flow cross-sectional area, A as functions of distance, x along the channel and time t. The equations can be given as:
Equation of mass

$$\frac{\partial A}{dt} + \frac{\partial Q}{\partial x} = q(x) \quad (1)$$

where the cross-sectional area of the flow is the flow rate and (Q) is the forcing term (i.e., precipitation, lateral flow).
Equation of momentum

$$\frac{1}{A}\frac{\partial Q}{\partial t} + \frac{1}{A}\frac{\partial}{\partial x}\left(\frac{Q^2}{A}\right) + g\frac{\partial y}{\partial x} - g\left(S_o - S_f\right) = 0 \quad (2)$$

where S_0 is the bed slope and S_f is the frictional slope, whilst *y* and *g* are the depth of water and gravitational pull, respectively. The complete form of Eq. (2) is termed as full dynamics equation. However, Eq. (2) can be further simplified if it is assumed that $S_0 = S_f$. This is known as the kinematic wave assumption. This condition can be equivalently expressed in Manning form as

$$A = \alpha Q^{\beta} \quad (3)$$

where

$$\alpha = \left(\eta P^{2/3} / \left(1.49\sqrt{S_o}\right)\right)^{0.6}$$

η = Manning roughness coefficient
P = wetted perimeter

S_o = bed slope
β = 0.6

Eq. (1) and (3) are the Saint Venant kinematic wave equations. By combining Eq. (1) and (3), the following equation can be obtained

$$\frac{\partial Q}{\partial t} + \frac{1}{\alpha\beta} Q^{(1-\beta)} \frac{\partial Q}{\partial x} = q \tag{4}$$

3.2 Weak Form of The Kinematic Wave Equation

The kinematic wave equation given by Eq. (4) can be solved numerically by converting the equation into weak form. This can be done by employing Galerkin weighted residual method. We first discretize Eq. (4) in time by forward difference to obtain

$$\frac{Q^{t+1} - Q^t}{\Delta t} + \frac{1}{\alpha\beta} Q^{(1-\beta)}, t + 1 \; \frac{\partial Q^{t+1}}{\partial x} = q^{t+1} \tag{5}$$

where t+1 and t refer to present and previous timestep, respectively. Rearranging gives

$$Q^{t+1} + \frac{\Delta t}{\alpha\beta} Q(1.\beta), t + 1 \frac{\partial Q^{t+1}}{\partial x} Q^t = q^{t+1} \tag{6}$$

By weighting Eq. (6) using shape functions, Ni and expressing the flow rate as Q = $N_j \hat{Q}_j$ where $\hat{Q}$ are the nodal values of Q, the following is obtained

$$\int_L N_i \left(N_j \hat{Q}_j + \frac{\Delta t}{\alpha\beta} N_k \hat{Q}_k^{(1-\beta)} \frac{\partial N_j \hat{Q}_j}{\partial x} - N_j \hat{Q}_j^{t} \right) dx = \int_L N_i \; q dx \tag{7}$$

To note, in Eq. (7), superscript t+1 is omitted for ease of notation. By collecting the nodal values, $\hat{Q}_j$ and shifting known terms to the right-hand side of the equation, Eq. (7) can now be given as

$$\left(\int_L N_i \; q dx + \int_L N_i \frac{\Delta t}{\alpha\beta} \left(N_k \hat{Q}_k \right)^{(1-\beta)} \frac{\partial N_j}{\partial x} dx \right) \hat{Q}_j = \int_L N_i \, N_j \, \hat{Q}_j^{t} \; dx + \int_L N_i \; q dx \tag{8}$$

Eq. (8) can be represented in matrix form as

$$\left[[M + K\left(\hat{Q}\right) \right] \left\{ \hat{Q} \right\} = -\{F\} \tag{9}$$

where [K] is the coefficient matrix, [M] is the mass matrix whilst $\{\hat{Q}\}$ and {F} are the vector of nodal values and nodal loads, respectively.

3.3 Nonlinear Solver

Eq. (9) is nonlinear thus requires a nonlinear solver. In this work, direct substitution scheme (also known as Picard direct substitution method) is employed. For mild nonlinearity the scheme works well.

3.4 Derivation of EFG Shape Functions

EFG uses moving least square (MLS) shape function as its interpolation function. MLS shape function are made of three components which are polynomial basis, weight function [W(x)] and non-constant coefficient {a(x)}.

$$[P|_n]^T\{a(x)\}^T - \{Q\}^T \neq 0 = \{R\} \tag{10}$$

where {R} is the vector residual of the right-hand side of Eq. (10). Due to this, the solution of the polynomial coefficient, a(x) is obtained by minimizing a potential, π given as

$$\pi = \{R\}[W]\{R\}^T \tag{11}$$

where [W] is a diagonal matrix of weight functions given as

$$[W] = \begin{bmatrix} W_1(x) & 0 & \cdots & 0 & 0 \\ 0 & W_2(x) & & 0 & 0 \\ \vdots & & \ddots & \vdots & \\ 0 & 0 & \cdots & W_{n-1}(x) & 0 \\ 0 & 0 & & 0 & W_n(x) \end{bmatrix} \tag{12}$$

By inserting Eq. (10) into Eq. (11) the following equation can be obtained

$$\pi = \left\{\{a(x)\}[P|_n]^T[W][P|_n]^T\{a(x)\}^T - 2\{a(x)\}[P|_n][W]\{Q\}^T + \{Q\}[W]\{Q\}^T\right\} \tag{13}$$

By minimizing Eq. (13) and setting it to zero would lead to

$$\frac{\partial \pi}{\partial\{a(x)\}} = \{2[P|_n][W][P|_n]^T\{a(x)\}^T - 2[P|_n][W]\{Q\}^T\} = 0 \tag{14}$$

Eq. (14) can be simplified into

$$[A]\{a(x)\}^T = [B]\{Q\}^T \tag{15}$$

where, [A] is the term of the weighted moment matrix which is as following

$$[A] = [P|_n][W][P|_n]^T \tag{16}$$

and [B] is given as

$$[B] = [P|_n][W] \tag{17}$$

The solution for {a(x)} T can be obtained by direct inverse of a [A]

$$\{a(x)\}^T = [A]^{-1}[B]\{Q\}^T \tag{18}$$

This would lead to the interpolation function

$$Q(x) = \{P\}[A]^{-1}[B]\{Q\}^T \tag{19}$$

From Eq. (19) the MLS shape function can be extracted as

$$\{N\} = \{P\}[A]^{-1}[B] \tag{20}$$

As given by Eq. (16) and (17), MLS requires the use of weighted function, [W(x)]. W can be given as

$$W = \begin{cases} \frac{2}{3} - 4\hat{r}_i^2 + 4\hat{r}_i^3 & \hat{r}_i \leq 0.5 \\ \frac{4}{3} - 4\hat{r}_i + 4\hat{r}_i^2 - \frac{4}{3}\hat{r}_i^3 & 0.5 < \hat{r}_i \leq 1 \\ 0 & \hat{r}_i > 1 \end{cases} \tag{21}$$

where

$$\hat{\mathrm{r}}_{\mathrm{i}} = \frac{\mathrm{d}_{\mathrm{i}}}{\mathrm{d}_{\mathrm{s}}} \tag{22}$$

where d_i is the distance from node to the point of interest and, d_s is the size of the support domain for the weighted function.

3.5 First Derivation of EFG MLS Shape Functions

The first derivation of MLS shape function can be obtained by rewriting Eq. (20) as

$$\{N\} = \{\alpha\}[B] \tag{23}$$

where

$$\{\alpha\} = \{P\}[A]^{-1} \tag{24}$$

Eq. (24) can be further arranged into

$$[A]\{\alpha\} = \{P\} \tag{25}$$

Eq. (25) can be differentiated using chain rule

$$[A]\left\{\frac{\partial \alpha}{\partial x}\right\} = \left\{\frac{\partial P}{\partial x}\right\} - \left\{\frac{\partial A}{\partial x}\right\}\{\alpha\} \tag{26}$$

From Eq. (25) the first derivative of {a} with respect to *x* can be established as

$$\left\{\frac{\partial a}{\partial x}\right\} = [A]^{-1}\left(\left\{\frac{\partial P}{\partial x}\right\} - \left[\frac{\partial A}{\partial x}\right]\{\alpha\}\right) \tag{27}$$

The first derivative of MLS shape function can be given by employing chain rule to Eq. (23)

$$\left\{\frac{\partial N}{\partial x}\right\} = \left\{\frac{\partial a}{\partial x}\right\}[B] + \{a\}\left[\frac{\partial B}{\partial x}\right] \tag{28}$$

By inserting Eq. (27) into Eq. (28) and differentiating matrix [B] with respect to x, the first derivative of MLS shape function can be obtained

4. Results and Discussion

The EFG formulation is verified against 2 benchmark to prove that the formulation is robust and conforms after which its optimal values for the shape function can be determined.

Benchmark 1: Verification against established benchmark of Chow *et.al.,* [6]

Chow *et.al.,* [6] is selected as the first verification benchmark for EFG. Chow uses FDM to obtain its numerical solution where the flow is driven by a time-varying inflow as given in Table 1. For this study is purely experimental the channel is neatly discretized into a finite grid system as shown in Figure 1. The channel has a bed slope of one percent and a Manning's roughness factor of 0.035. There is no lateral flow or rainfall. The initial condition is a uniform flow of 2000 cfs along the channel.

Table 1
Time varying flow data from Chow *et.al.,* [6]

Inflow time (min)	Inflow rate (cfs)
0	2000
12	2000
24	3000
36	4000
48	5000
60	6000
72	5000
84	4000
96	3000
108	2000
120	2000

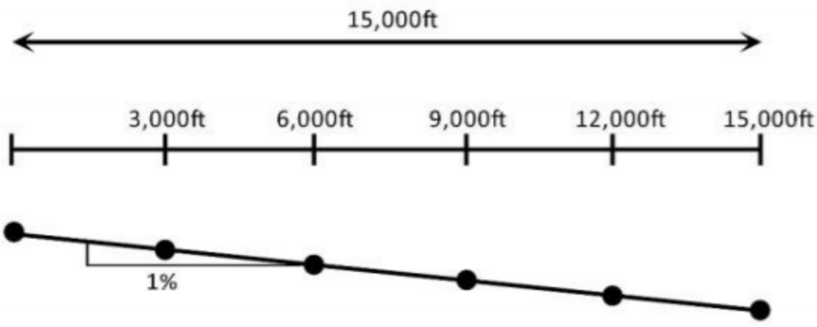

Fig. 1. The neatly discretized hypothetical channel by Chow *et.al.,* [6]

Figure 2(a) shows the plot of flow rate, calculated at various locations whilst Figure 2(b) shows the plot of a distance of 6000 ft from upstream. In the latter, close agreement can be observed between the results given by EFG and the one given by Chow et.al., [6]. It can also be seen that the EFG solution converges with the increase in the number of nodes.

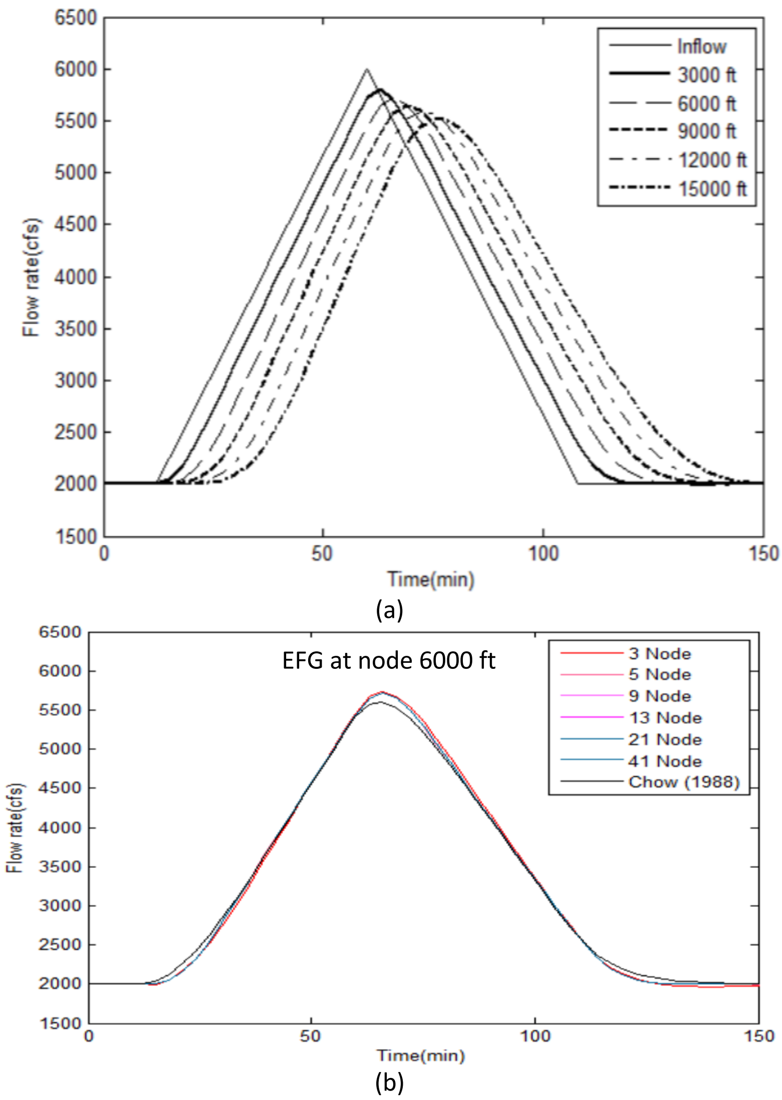

Fig. 2. Flow rate validation for Benchmark 1

Case 2: Verification against physical gauged data by Litrico *et al.,* [8] Unlike Chows experimental benchmark, Litrico *et al.,* [8] benchmark is data actual dataset gauged from Jacui River in Brazil (refer to Figure 3). Its flow is more varying and is driven by time-varying upstream boundary conditions. This is controlled by the upstream controlled discharge of the dam Jacui River in Brazil between Itauba and Volta Grande, recorded at a time step of 30 minutes. Table 2 gives the data for the river.

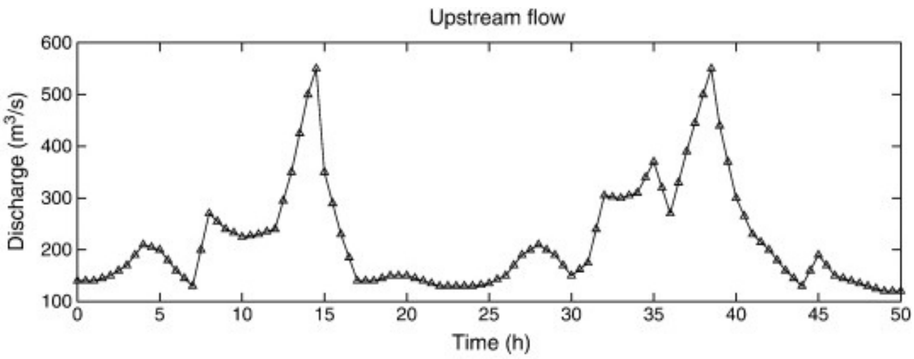

Fig. 3. Varying Upstream flow of Jacui River from Litrico *et al.,* [8]

Table 2
Physical dimensions of Jacui River from Litrico *et al.,* [8]

Data	Value
Channel length (L)	29600 m
Width (W)	55.6 m
Manning coefficient (n)	0.07
Slope (Sb)	0.00089

Figure 4 shows the plot of the flow rates where a similar trend of prediction is given by both numerical methods plotted against the gauged data. It shows that EFG formulation is in close agreement between the 2 benchmark values thus validates this formulation. There are slight differences in some of the values due to the assumptions made in shape parameters in EFG. Next, the optimum value of the shape parameters will be determined and then used in the convergence study.

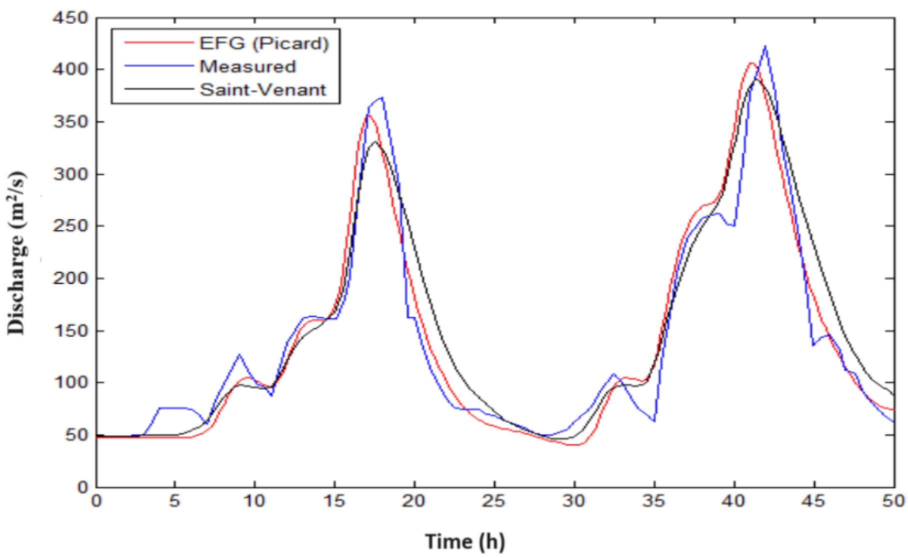

Fig. 4. Flow rate validation for Benchmark 2

4.1 Analytical Procedure for The Determination of Optimal Shape Parameters Values

The usage of suitable shape parameters value in analysis is critical for the best execution rate and the accuracy of a formulation (Liu and Gu, 2005). By adopting moving least squares (MLS) as the interpolation function, the specification of two shape parameters, and is required which values are best determined by conducting a numerical test. Optimum values are taken as those that provide the lowest error norms which can be calculated as

$$e = \frac{1}{N}\sum_{j}^{N} \frac{\left|u(x_j)^{EFG} - u(x_j)^{FEM}\right|}{\left|u(x_j)^{FEM}\right|} \tag{29}$$

where N is the number of results considered whilst $u(x_J)^{EFG}$ and $u(x_J)^{FEM}$ are the values of flow rates obtained from EFG and FEM respectively.

Eq. (29) is a L2-norm loss function formulation also called least square error (LSE). The basic idea of this formulation is to minimize the sum of the square of differences between the target values and the estimated values.

Since there is no closed-form solution available for the two benchmark cases, the “accurate” solution herein, i.e $u(x_J)^{FEM}$ is taken as the converged value from FEM formulation.

The optimum value of as is shown in Figure 5 where the error norms of the flow rates from the benchmark cases for varying values of shape parameter and numbers of nodes (i.e., 11, 21 and 41). From the plots, it is evident that EFG has lower error norms for higher node numbers. While the results seem to be insensitive for Case 1 (Chow), there is a slight reduction in the error norms for Case 2. Narrowing the range of the reduction in between 1 and 2, the optimum value for as is chosen as 1.

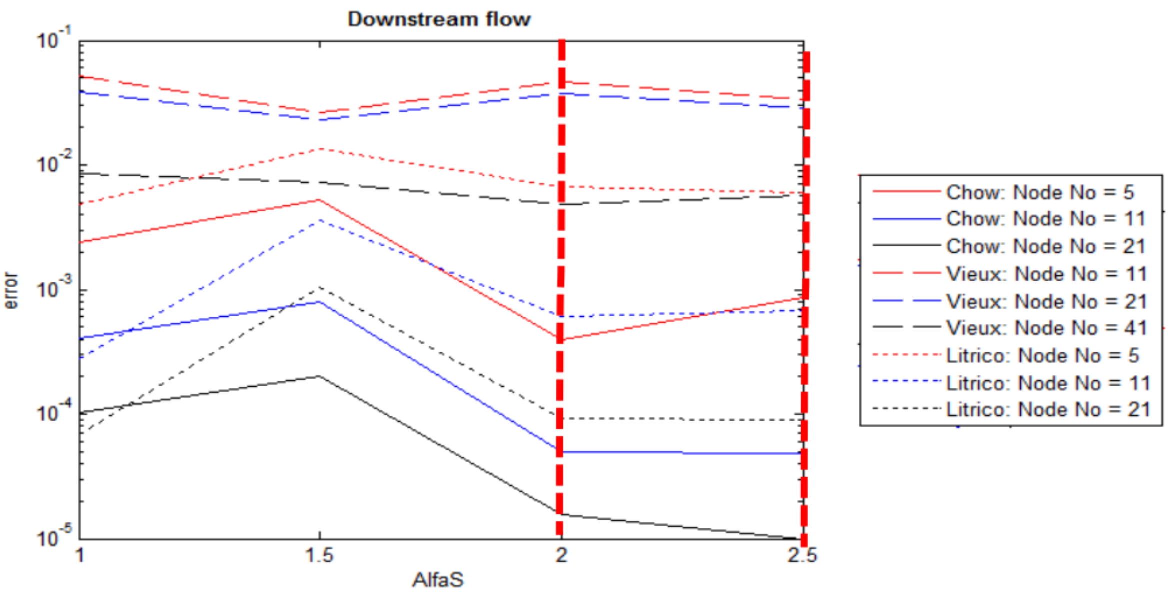

Fig. 5. Optimum value determination for shape parameter a_S

Having determined the optimum value of as, the optimum value for GP, is then determined. Similar trend is observed where there is a slight reduction in error norms for Case 2 as shown in Figure 6. Narrowing the range of the reduction in between 2 and 3, the optimum value for GP is chosen as 2.

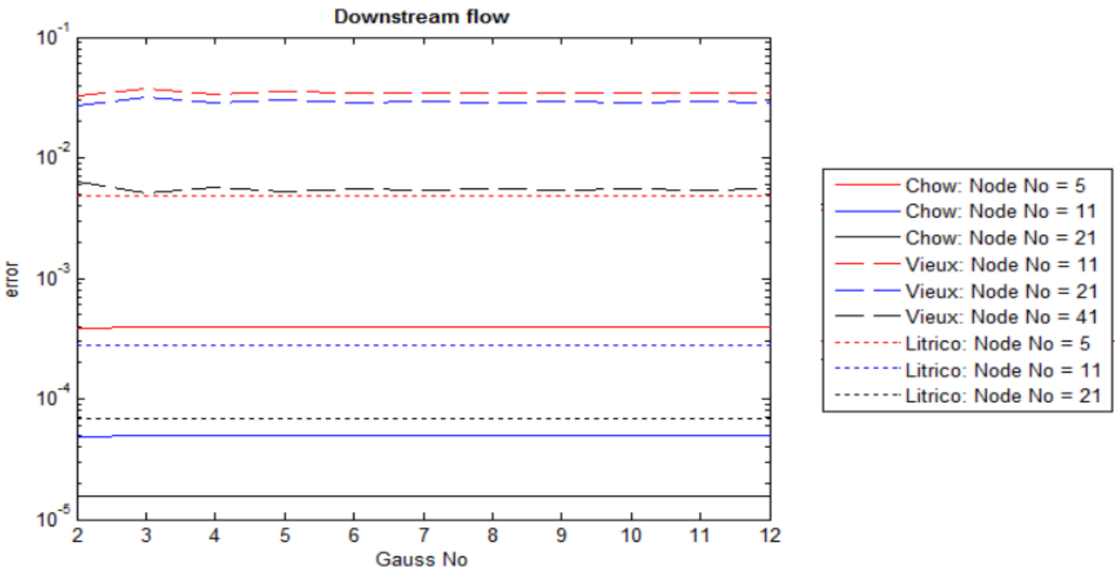

Fig. 6. Optimum value determination for the shape parameter GP

4.2 Determining Convergence of The Numerical Performance

Convergence study is vital for numerical method research to determine the performance of a newly derived formulation. Performance of the formulation is measured by measuring convergence rate which is the speed at which the formulation can arrive at the "correct" form. Numerical performance of EFG is assessed by comparing its convergence rate against FEM and FDM. To ensure that EFG performs at its best, optimum values from previous tests are used.

By referring to Figures 7 and 8, the different performance between the weighted-residual based formulations (FEM and EFG) and the collocation based FDM is apparent where the formers converge faster than the latter despite all being of 1st order accuracy. It is well known that the averaging of the error inherent in the weighted residual formulation would lead to a better performance. In this context, EFG performs identical to FEM and better than FDM. This highlights the potential of EFG as an alternative numerical method to FEM for hydrologic modelling as the method, whilst has equal performance, does not require the formation of mesh and assembly process.

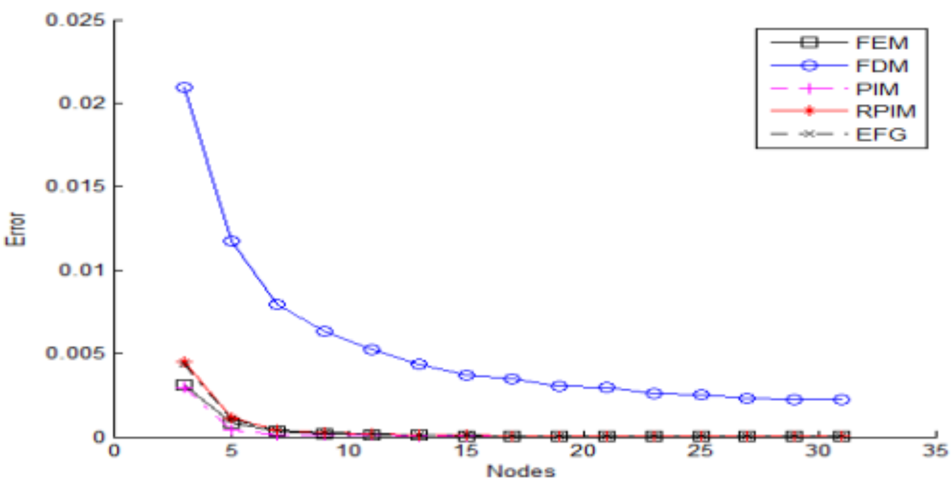

Fig. 7. Convergence rate for Benchmark 1

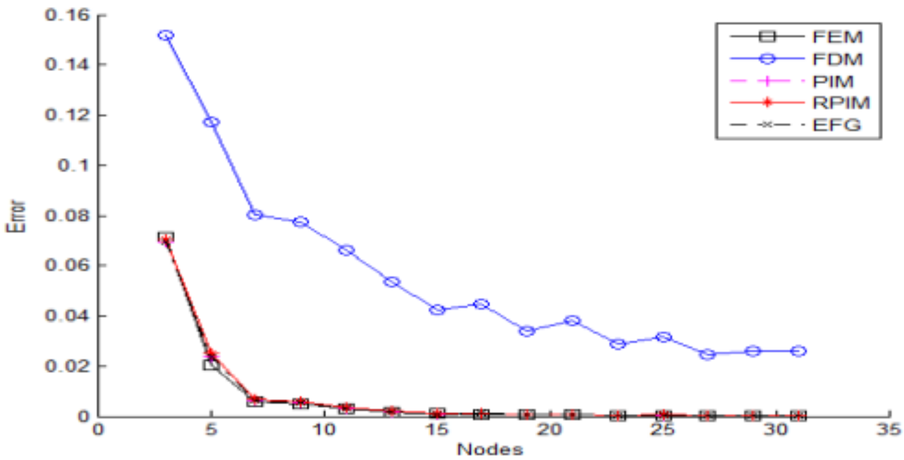

Fig. 8. Convergence rate for Benchmark 2

5. Conclusions

The discussion in this paper details the solving of Saint Venant kinematic wave equation using EFG formulation. The effectiveness of the EFG formulation is tested against various benchmark problems. To gauge the performance of EFG method its optimum shape parameter values are determined by optimising via a numerical test. Using the optimum shape values found, EFG formulation is found to perform better than FDM and on par with FEM in a convergence study. Therefore, EFG shows potential as a numerical method which could be used for hydrological modelling with its benefits of not needing a mesh to be formed and its assembly process.

Funding information

The authors would like to thank the Ministry of Higher Education of Malaysia for the financial funding of this project under R.J130000.7851.5F122, the Research Management Centre (RMC) of Universiti Teknologi Malaysia, Ikohza SEIR Malaysia Japanese International Institute of Technology UTM, UTM for their support for the research management

References

[1] Singh, Vijay P. "Kinematic wave modeling in hydrology." In *World Water & Environmental Resources Congress 2003*, pp. 1-38. 2003. https://doi.org/10.1061/40685(2003)165

[2] Parlange, J-Y., C. W. Rose, and G. Sander. "Kinematic flow approximation of runoff on a plane: An exact analytical solution." *Journal of Hydrology* 52, no. 1-2 (1981): 171-176. https://doi.org/10.1016/0022-1694(81)90104-9

[3] Hjelmfelt Jr, Allen T. "Overland flow from time-distributed rainfall." *Journal of the Hydraulics Division* 107, no. 2 (1981): 227-238. https://doi.org/10.1061/JYCEAJ.0005613

[4] Govindaraju, R. S., S. E. Jones, and M. L. Kavvas. "On the diffusion wave model for overland flow: 1. Solution for steep slopes." *Water Resources Research* 24, no. 5 (1988): 734-744. https://doi.org/10.1029/WR024i005p00734

[5] Govindaraju, R. S., M. L. Kavvas, and S. E. Jones. "Approximate analytical solutions for overland flows." *Water resources research* 26, no. 12 (1990): 2903-2912. https://doi.org/10.1029/WR026i012p02903

[6] Chow, V. T., Maidment, D. R., & Mays, L. W. (1988, February 1). Applied Hydrology. McGraw-Hill Science, Engineering & Mathematics.

[7] Vieux, Baxter E., Vincent F. Bralts, Larry J. Segerlind, and Roger B. Wallace. "Finite element watershed modeling: one-dimensional elements." *Journal of water resources planning and management* 116, no. 6 (1990): 803-819. https://doi.org/10.1061/(ASCE)0733-9496(1990)116:6(803)

[8] Litrico, Xavier, Jean-Baptiste Pomet, and Vincent Guinot. "Simplified nonlinear modeling of river flow routing." *Advances in Water Resources* 33, no. 9 (2010): 1015-1023. https://doi.org/10.1016/j.advwatres.2010.06.004

[9] Liu, Gui-Rong, and D. Karamanlidis. "Mesh free methods: moving beyond the finite element method." *Appl. Mech. Rev.* 56, no. 2 (2003): B17-B18. https://doi.org/10.1115/1.1553432

[10] Liu, Gui-Rong, and Yuan-Tong Gu. *An introduction to meshfree methods and their programming*. Springer Science & Business Media, 2005.

[11] Belytschko, Ted, Yun Yun Lu, and Lei Gu. "Element-free Galerkin methods." *International journal for numerical methods in engineering* 37, no. 2 (1994): 229-256. https://doi.org/10.1002/nme.1620370205

[12] Belytschko, T., P. Krysl, and Y. Krongauz. "A three-dimensional explicit element-free galerkin method." *International Journal for Numerical Methods in Fluids* 24, no. 12 (1997): 1253-1270. https://doi.org/10.1002/(SICI)1097-0363(199706)24:12<1253::AID-FLD558>3.0.CO;2-Z

[13] Krysl, Petr, and Ted Belytschko. "The element free Galerkin method for dynamic propagation of arbitrary 3-D cracks." *International Journal for Numerical Methods in Engineering* 44, no. 6 (1999): 767-800. https://doi.org/10.1002/(SICI)1097-0207(19990228)44:6<767::AID-NME524>3.0.CO;2-G

[14] Chen, X. L., G. R. Liu, and S. P. Lim. "An element free Galerkin method for the free vibration analysis of composite laminates of complicated shape." *Composite Structures* 59, no. 2 (2003): 279-289. https://doi.org/10.1016/S0263-8223(02)00034-X

[15] Hirol, H. "Meshfree Formulations of Kinematic Wave for Channel Flow Routing." PhD diss., Ph. D. Universiti Teknologi Malaysia, Malaysia, 2016.

[16] Hirol, H., M. A. M. Noor, E. H. Kasiman, A. K. B. Hong, Z. Yusop, and A. Y. M. Yassin. "Meshless point interpolation formulation of kinematic wave equation for flood routing." *Journal of Engineering and Applied Sciences* 12, no. 20 (2017): 5286-5293.

[17] Dehghan, Mehdi, and Mostafa Abbaszadeh. "Proper orthogonal decomposition variational multiscale element free Galerkin (POD-VMEFG) meshless method for solving incompressible Navier–Stokes equation." *Computer Methods in Applied Mechanics and Engineering* 311 (2016): 856-888. https://doi.org/10.1016/j.cma.2016.09.008

[18] Chowdhury, Habibullah Amin, Adam Wittek, Karol Miller, and Grand Roman Joldes. "An element free Galerkin method based on the modified moving least squares approximation." *Journal of Scientific Computing* 71 (2017): 1197-1211. https://doi.org/10.1007/s10915-016-0337-z

[19] Zeifang, Jonas, and Jochen Schütz. "Implicit two-derivative deferred correction time discretization for the discontinuous Galerkin method." *Journal of Computational Physics* 464 (2022): 111353. https://doi.org/10.1016/j.jcp.2022.111353

[20] Li, Xiaolin, and Shuling Li. "Analysis of an element-free Galerkin method for the nonlinear Schrödinger equation." *Mathematics and Computers in Simulation* 203 (2023): 538-552. https://doi.org/10.1016/j.matcom.2022.06.031

[21] Smith, Stephen P., Gary H. Menary, James Nixon, and Brian G. Falzon. "Numerical and experimental validation of an explicit meshfree method: With applications to material forming." *Engineering Analysis with Boundary Elements* 122 (2021): 43-61. https://doi.org/10.1016/j.enganabound.2020.10.013

[22] Barre, DE SAINT-VENANT. "Theory of unsteady water flow, with application to river floods and to propagation of tides in river channels." *French Academy of Science* 73 (1871): 148-154.